PAGEOPH, Vol. 123 (1985) 0033-4553/85/010059-22$1.50 + 0.20/0

Design Parameters for Borehole Strain Instrumentation

MICHAEL T. GLADWIN[1] AND RHODES HART[1]

Abstract—The response of a borehole strain meter to hydrostatic and shear deformations in an isotropic medium is calculated to facilitate optimum instrument design and produce instrument response factors for parameters typically encountered in installed instruments. Results for an empty borehole are first compared with results for an instrument in intimate contact with the surrounding rock. The effects of the grout used to install the instrument are then examined. Where possible, analytic forms for the response factors are given. Results for typical installations are then presented in graphical form for optimizing instrument design in an environment of known elastic parameters. Alternatively, the results may be applied in the measurement of unknown strain signals, to correct for instrument response or to provide in-situ estimates of the elastic properties of the environment by examination of observed strain response to known strain signals.

Key words: Borehole strain; strain monitoring; shear stran; earthquake strain.

Introduction

An important recent development in earth strain monitoring studies is the realization that to reliably monitor the small strains encountered and to avoid extensive contamination of the record with near-surface disturbances, strain meters should be installed at depths of at least one hundred metres in competent rock. Borehole hydrostatic-strain instruments have been in operation for more than ten years (SACKS *et al.*, 1971), and recently two instruments capable of measuring both hydrostatic and shear strain have been installed in California (GLADWIN, 1984). The latter instruments resolve strain to 30 picostrain in the horizontal plane by three measurements (in the typical strain rosette pattern) of the radial deformation of a cylinder wall grouted into the borehole with expanding cement. This paper provides an understanding of the isotropic elastic behavior of such inclusions for calculation of the far-field strains in the host rock from the observed cylinder deformations, and for optimising the design of such instruments. A previous derivation (JAEGER and COOK, 1976, chap. 10.4) considers a single inclusion in horizontal boreholes. SAKATA *et al.* (1982) mention the effect of the grout but do not explicitly include it in their solutions. Omission of the effects of the grout limits the usefulness of their solutions. The effect of anisotropy of the host rock on the stresses in a borehole with a single inclusion has been examined

[1] Department of Physics, University of Queensland, St. Lucia, 4067, Australia.

by AMADEI (1983). Such effects, though no doubt significant in many practical situations, are not included in this analysis, but are not a first priority for treatment of actual installed instruments.

Observed deformations of the inner wall of an instrument grouted in a hole are determined by the elastic moduli of the surrounding rock, the grout material, and the material of which the instrument is made, the diameter of the borehole and the instrument package, and the wall thickness of the instrument. For insight into the effects of these nine parameters three increasingly complex models are examined. The first introduces the nomenclature chosen and provides a description of the deformation of the wall of an empty borehole. The second model, the single-ring model, considers the effect of installing an instrument with annular cross-ection in intimate contact with the rock. The third model presents the effects of a grout introduced between the instrument and the rock wall. This two-ring model is a critical case for downhole strain instrumentation since grouts are commonly used for coupling and preload for the instrument implant.

The paper divides into two sections. In the first section the equations describing the instrument behaviour for each of the models are derived. These are then used in the second section to illustrate in graphical form the instrument response for typical parameters encountered. This graphical presentation becomes necessary because there are many complex interactions of the nine basic parameters involved and because it is not feasible to present analytic solutions in sufficiently concise and usable form. Scaled moduli and instrument geometries are used on all graphs so that they may be applied directly in instrument design or in inversion of observed data to remote strain fields.

Section 1. Theory

A. Introduction

There are two stages in the derivation of far-field strain in the host rock from measurements of the radial deformation of the instrument wall. The first derives the radial deformation U_r of the inner instrument wall expressed as a function of the far-field principal strains in the rock and the angle between the radius where the deformation is observed and the axis of maximum compression. This function will have as parameters the elastic constants of the instrument, the grout, and the rock, and the hole and instrument radii. In the second stage the set of three such equations for observations of radial deformation at three different points spaced 60 degrees apart is inverted so as to express the principal strains and their direction as functions of the three observations.

For strains measured in the plane perpendicular to a vertical borehole, the

boundary condition imposed on the vertical dimension is significant. In the present analysis the assumption of plane stress for stress changes has been made, where stress is considered constant in the vertical direction owing to the presence of the nearby free surface. Results for the plane-strain assumption may be derived from the present analysis by modification of the parameter χ, as noted below.

B. Conventions and symbols

In this work the elasticity convention of compression as negative strain will be used, and the X axis will be fixed as the axis of maximum compression.

Regions of the installed instrument are numbered as follows: *1*, instrument; *2*, grout; *3*, rock.

The following symbols are used.

R_i	Inner radius of region i
N_i	R_3/R_i; e.g., N_1 is the ratio of hole radius to instrument inner-wall radius
E_i	Young's modulus
K_i	Bulk modulus
G_i	Rigidity
ν_i	Poisson's ratio
χ	$(3-\nu)/(1+\nu)$ for plane stress; $(3-4\nu)$ for plane strain
U_r	Radial displacement
θ	Angle measured clockwise from the axis of maximum compression
σ	Principal stress
ε	Principal strain
P	Uniaxial stress
V	Areal stress $= (\sigma_1+\sigma_2)/2$; for plane stress V = volumetric stress
S	Shear stress $= (\sigma_1-\sigma_2)/2$
v	Areal strain $= (\varepsilon_1+\varepsilon_2)/2$; planar hydrostatic strain.
Δ	Dilation strain; for plane stress $\Delta = 2v(1-2\nu)/(1-\nu)$
s	Shear strain $= -(\varepsilon_1-\varepsilon_2)/2$

C. Basic theory

For each model it will be shown that the radial displacement of the instrument's inner wall at angle θ clockwise from a uniaxial stress P applied at a large distance compared with the borehole diameter can be expressed as

$$U_r(r_1) = R_1 P/8G_1(a + b\cos 2\theta) \tag{1}$$

where a and b are dimensionless constants, functions of the elastic constants and the radii.

The displacement arising from principal stresses σ_1 and σ_2, where σ_1 is the principal stress of maximum compression (most negative) and θ is measured clockwise from above from the X axis, is then given by

$$\begin{aligned} U_r(R_1) &= (R_1/8G_1)[a(\sigma_1 + \sigma_2) + b(\sigma_1 - \sigma_2)\cos 2\theta] \\ &= (R_1/4G_1)(aV - bS\cos 2\theta) \end{aligned} \tag{2}$$

The apparent instrument in-situ bulk and shear moduli, K and G, defined as

$$K = \frac{V}{3U_r/R_1} \quad \text{for} \quad S = 0 \tag{3}$$

$$G = \frac{S}{U_r/R_1} \quad \text{for} \quad V = 0 \tag{4}$$

are then calculated from equation 2 to be

$$K = 4G_1/3a \tag{5}$$

$$G = 4G_1/b \tag{6}$$

For plane stress, areal and shear stresses are related to equivalent strains by the equations

$$V = 2\frac{(1 + \nu_3)}{(1 - \nu_3)}G_3 v \tag{7}$$

$$S = 2G_3 s \tag{8}$$

By means of equations 7 and 8 the radial displacement in equation 2 can be expressed in terms of the areal and shear strains as

$$U_r = R_1(cv - ds\cos 2\theta) \tag{9}$$

where

$$c = \frac{a(1 + \nu_3)G_3}{2(1 - \nu_3)G_1} \tag{10}$$

$$d = \frac{bG_3}{2G_1} \tag{11}$$

The constants c and d of equation 9 may be viewed as the hydrostatic and shear response factors for the in-situ instrument.

From equation 9 we have the following for three measurements of radial deformation U_i. Note that U_1 is measured at angle θ clockwise from above from the axis of maximum compression and that U_2 and U_3 are measured 60 and 120 degrees, respectively, from U_1, clockwise.

$$U_1 = R_1(cv - ds\cos 2\theta) \tag{12}$$

$$U_2 = R_1(cv - ds(-1/2 \cos 2\theta - \sqrt{3}/2 \sin 2\theta)) \tag{13}$$

$$U_3 = R_1(cv - ds(-1/2 \cos 2\theta + \sqrt{3}/2 \sin 2\theta)) \tag{14}$$

These equations are easily inverted to express v, s, and θ in terms of U_1, U_2, and U_3 as

$$v = \frac{1}{c}\frac{(U_1 + U_2 + U_3)}{3R_1} \tag{15}$$

$$\theta = 1/2 \tan^{-1}\left(\frac{\sqrt{3}(U_3 - U_2)}{(U_1 - U_2) + (U_1 - U_3)}\right) \tag{16}$$

$$s = \frac{\sqrt{2}}{d3R_1}\sqrt{[(U_1 - U_2)^2 + (U_2 - U_3)^2 + (U_3 - U_1)^2]} \tag{17}$$

$$= \frac{-(U_3 - U_2)}{dR_1\sqrt{3} \sin 2\theta}$$

Two conventions are possible for uniquely specifying s and θ. If s is kept positive, θ can be limited to -90 to $+90$ degrees, and the sense of the shear is seen in the rotation of the axis of maximum compression. Alternatively, the sense of the shear can be incorporated in s by being allowed it to change sign, in which case θ is restricted to the range -45 to 45 degrees and does not refer to the axis of maximum compression. The second convention proves to be the easier to use in practical earth-strain monitoring.

The following observations apply to equations 15 to 17, for cases where radial deformation can be expressed in the form of equation 1.

1. The areal strain is obtained from the apparent instrument areal strain $(U_1 + U_2 + U_3)/3R_1$ by scaling with the instrument response factor c (see equation 10).

2. The angle θ is independent of the gain factors c and d and therefore independent of the model used.

3. The far-field strain is obtained from the apparent instrument shear strain $\sqrt{2}[(U_1 - U_2)^2 + (U_2 - U_3)^2 + (U_3 - U_1)^2]^{1/2}/(3R_1)$ by scaling with the instrument strain gain factor d (see equation 11).

As a reference point it is useful to have the results for undisturbed rock under plane strain. Here

$$U_r = R_1(v - s \cos 2\theta) \tag{18}$$

so that from equation 9 it is seen that $c = d = 1$, and hence the identification of c and d as instrument strain response factors. Using equations 10 and 11 in equations 5 and 6 gives the effective instrument moduli for this case as

$$K = \frac{(1 - 2\nu_3)}{(1 - \nu_3)}K_3 \tag{19}$$

$$G = 2G_3 \tag{20}$$

Thus the rock is softer to compression under plane-stress conditions than in a homogeneous stress, but unchanged under shear strain.

D. Models

1. The empty borehole Analysis of the empty borehole is useful when the instrument is very much softer than the surrounding rock, so that the instrument deformation follows the deformation of the hole wall. The radial deformation in such cases is well known (for example, equation 21 of section 10.4 of JAEGER and COOK, 1976), and for the case of plane stress it reduces to

$$U_r = (R_1 P/8G_3)(\chi_3 + 1)(1 + 2\cos 2\theta) \tag{21}$$

By comparing this equation with equation 1 we identify a and b for this case as

$$a = 4/(1 + \nu_3) \tag{22}$$

$$b = 8/(1 + \nu_3) \tag{23}$$

and from equations 10 and 11

$$c = 2/(1 - \nu_3) \tag{24}$$

$$d = 4/(1 + \nu_3) \tag{25}$$

Here the instrument response factors are independent of the rigidity of the rock and the borehole radius and are somewhat dependent on Poisson's ratio for the rock. The apparent instrument moduli for this case are, from equations 5 and 6,

$$K = \frac{(1 - 2\nu_3)}{2} K_3 \tag{26}$$

$$G = \frac{(1 + \nu_3)}{2} G_3 \tag{27}$$

and are softer than the undisturbed rock (equations 19 and 20).

2. The one-ring model This case models situations where the grout is negligibly thick, or where the grout has elastic properties identical with the host rock. The model used is that of a single ring welded in an infinite plate, and the solution is essentially provided in SAVIN (1961, Chap. 5). It is treated separately here from the more general two-ring model bcause a simpler analytical result ensues.

The constants a and b of equation 1 can be expressed as

$$a = a_1(\chi_1 - 1) + b_{-1}N_1^2 \tag{28}$$

$$b = a_3(\chi_1 - 3)N_1^{-2} + b_1 + a_{-1}(\chi_1 + 1)N_1^2 + b_{-3}N_1^4 \tag{29}$$

where a_i and b_i are functions, given in Appendix A, of the ring radii and the elastic constants of the rock and of the ring, and where $N_1 = R_3/R_1$. With these equations the instrument response factors c and d can be obtained from equations 10 and 11. Examination of the result reveals the following.

1. For $G_3 = G_1$ and $v_3 = v_1$ the results reduce to those of the empty borehole.
2. For $R_3 = R_1$ the results again reduce to the empty-borehole case.
3. The rigidity of the ring and the rock enter the result only as the ratio G_3/G_1.
4. The ring radii enter the result only as the ratio R_3/R_1.

3. The two-ring model In this case the effect of the grout is included in a model consisting of two rings welded concentrically in a hole in an infinite plate. The inner ring represents the instrument wall, and the second ring represents the grout. The more general n-ring case has been solved by SAVIN (1961, see Chap. 5). However, six errors in his solution (at equations 5.8) and the complexity of the expansion of his result have made it necessary to rederive the solution to obtain a useful set of design equations. An outline of this derivation is given in Appendix B.

The coefficients a and b of equation 1 are found to be

$$a = 4[1 - \chi_1)a_1^1 - b_{-1}^1 N_1^2] \tag{30}$$

$$b = 4[-a_{-1}^1 N_1^2(1 + \chi_1) + \frac{a_3^1}{N_1^2}(3 - \chi_1) - b_{-3}^1 N_1^4 - b_1^1] \tag{31}$$

where the a_j^1 and b_j^1 are members of a set of 22 complex quantities which satisfy the set of 22 complex linear equations given in Appendix B. They are functions of the Poisson ratios for each of the three regions and the radius ratios

$$N_1 = R_3/R_1$$

$$N_2 = R_3/R_2$$

and the rigidity ratios

$$e_{21} = G_2/G_1$$

$$e_{31} = G_3/G_1$$

This set of equations can be inverted numerically to obtain the coefficients in equations 30 and 31. The instrument response factors c and d are then obtained from equations 10 and 11.

Section 2. Typical instrument response

In this section the instrument response to strains in the host rock is calculated for the three models presented in the first section, for typical values encountered in practical instruments in the field.

Range of parameters

For an examination of the interaction of the various parameters involved in these solutions a set of parameters has been chosen close to those used in instruments installed in California (GLADWIN, 1984). The results of the various models will be presented graphically as a series of parametric curves for each variable of interest over a range of the independent variable which encompasses typical values for similar installations. Where specific numerical values are needed for concise presentation of results in this form, the parameters of this instrument will be used ($G_1 = 83.9$ GPa and $\nu_1 = 0.283$), but in all cases the results can be scaled to other instrument geometries. Where possible all parameters are normalised as ratios.

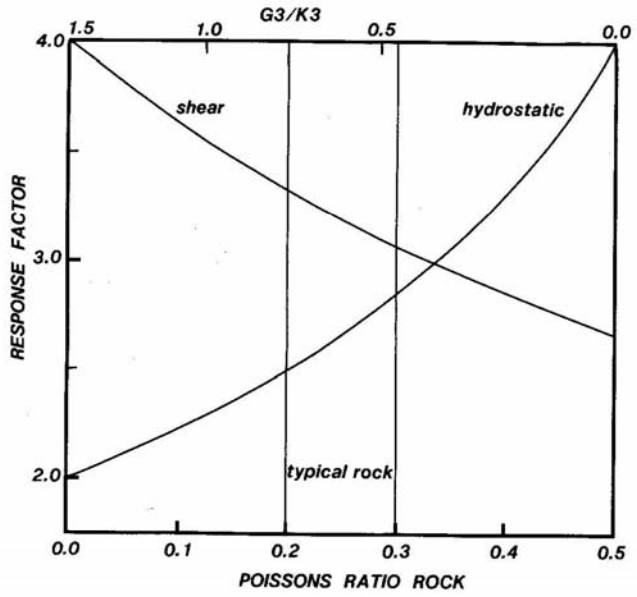

Figure 1
The dependence of the strain response factors on Poisson's ratio for an empty borehole under plane stress. The response factors are independent of other parameters. The top scale expresses the dependence in terms of the ratio of the rigidity modulus of the rock (G_3) to the bulk modulus (K_3). Values encountered for typical rock are indicated.

The empty borehole

The strain response factors are given by equations 24 and 25 and are plotted in Figure 1 as a function of Poisson's ratio for the rock. The scale shown at the top of the figure in terms of G/K is useful in understanding the dependence of these response factors on rock moduli. Thus a borehole in rock enhances the radial deformations from the far-field strains by unequal factors of roughly 3 for typical rocks. Maximum enhancement is 4 in both cases, with a minimum enhancement of 2 for hydrostatic strains and 2.67 for shear strains. The response factors are equal only for ν_3 equal to 1/3, where their value is 3. A range of Poisson's ratio for typical rocks is indicated.

The one-ring model

The response factors for this model are given by equations 10 and 11, with equations 28 and 29 for a and b, and are functions of the ratio of the rigidity moduli

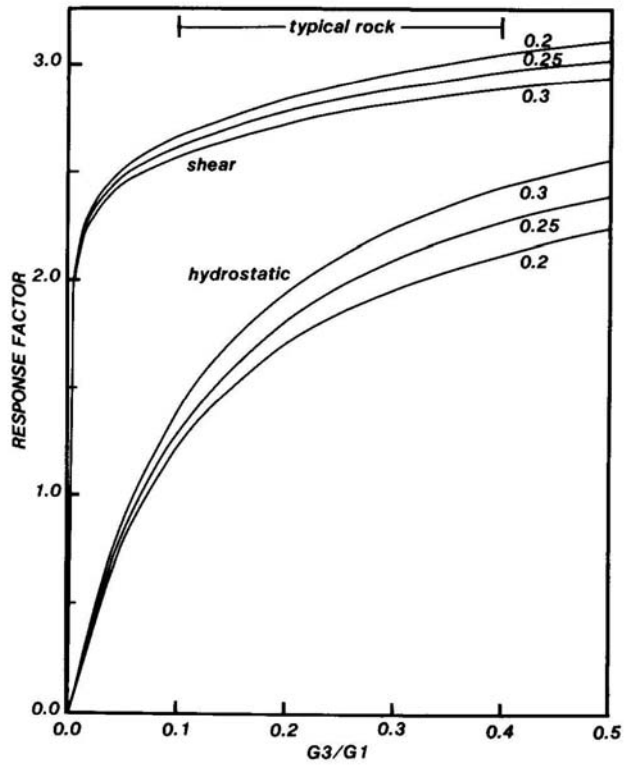

Figure 2

The dependence of the strain response factors on the rock rigidity (expressed as a ratio of rock-to-instrument rigidity, G_3/G_1) for the one-ring model for a stainless-steel instrument in intimate contact with the borehole wall with wall thickness 9% of the borehole radius. Curves for the Poisson ratio of the rock from 0.2 to 0.3 (covering the normal range of rock) show that it has minimal and opposite effects for hydrostatic and shear response.

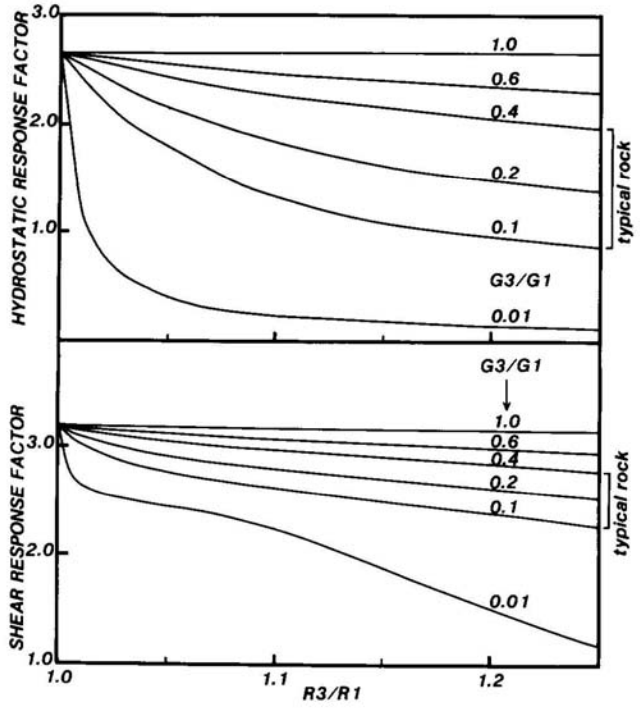

Figure 3

The dependence of the hydrostatic and shear response factors on the ratio of the outer (R_3) and inner (R_1) instrument radii for the one-ring model. Several curves are shown for a range of rock rigidity of 0.01 to 1.0 of the instrument rigidity, with a region of typical rock rigidity indicated. As the radii ratio approaches 1 or the rock modulus approaches that of the instrument material, the responses tend to those of the empty borehole, small differences being due to differences in poisson's ratio. For rock 'softer' than the instrument, increasing the instrument wall thickness decreases the responses more significantly for 'softer' rock.

of the host rock and the material of the instrument, G_3/G_1, the Poisson ratios ν_1 and ν_3, and the radii ratio R_3/R_1. Figure 2 shows the variation of the response factors with the rigidity ratio, for $R_3/R_1 = 1.11$ corresponding to installed stainless-steel borehole instruments, with Poisson's ratio of the rock equal to 0.25. For a typical rock modulus (21 GPa) the response factors are 2.0 and 2.8 respectively. Shear response is always greater than hydrostatic response; that is, the hole is stronger in compression than it is in shear, and as the rock rigidity decreases, the shear response decreases at a slower rate, so that there is still significant shear response at $G_3/G_1 = 0.03$ when the hydrostatic response has dropped to 0.6. A region of typical rock shear modulus (7 to 30 GPa) is indicated.

The variation of the response factors with instrument wall thickness (expressed as the ratio R_3/R_1) is shown in Figure 3 with the rigidity ratio G_3/G_1 as a parameter and $\nu_3 = 0.25$. The values obtained for $R_3/R_1 = 1$ correspond to those for the empty borehole, and for $G_3/G_1 = 1$ there is only slight dependence on the radius ratio, this arising from the different Poisson ratios for the instrument and the rock. In general, increasing the radius ratio (increasing the instrument wall thickness) decreases the

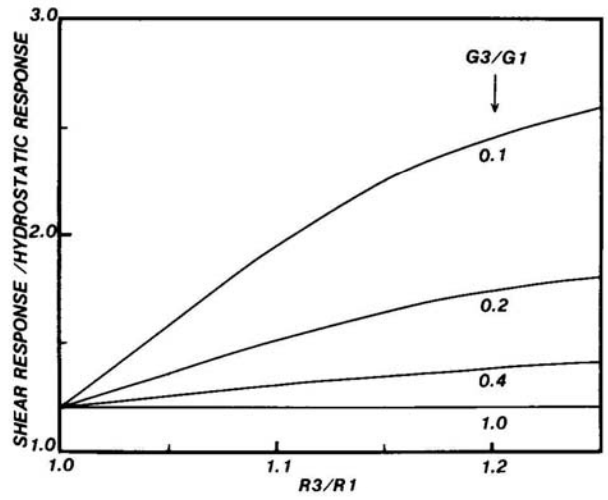

Figure 4

The ratio of shear to hydrostatic response factors as a function of the ratio of outer to inner radii of the instrument, showing, for rock rigidity less than the instrument material rigidity, significant enhancements of the shear response over the hydrostatic response. Poisson's ratio for the rock is 0.25.

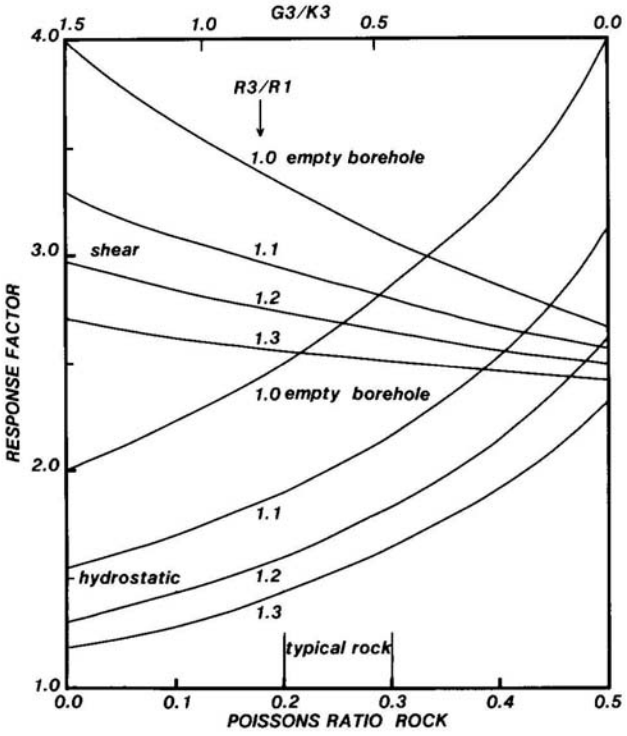

Figure 5

The effect of the Poisson ratio of the rock on the response factors for the one-ring model for various values of the ratio of instrument outer (R_3) to inner (R_1) radii. The empty-borehole curves (where $R_3/R_1 = 1$) and a region of typical-rock Poisson ratio are shown. Increasing Poisson's ratio increases the hydrostatic response but decreases the shear response. For all curves $G_3/G_1 = 0.26$; that is, the rock rigidity is approximately 22 GPa.

responses for rigidity ratios less than 1, and this decrease is more pronounced for the hydrostatic response factor. The shear response can thus be enhanced relative to the hydrostatic response by increasing the instrument wall thickness, as is shown in Figure 4, with larger enhancements possible for 'softer' rock. These results can be related to a cylinder's being stronger in compression than in shear.

Figure 5 shows the effect of the Poisson ratio of the rock on the response factors for several radius ratios and for $G_3/G_1 = 0.26$. The effect is similar to that encountered in an empty borehole (see Figure 1).

The two-ring model

The instrument response factors for this model are given by equation 10 and 11, with equations 30 and 31 for the values of a and b, and are functions of the rigidity ratios G_2/G_1 and G_3/G_1, Poisson's ratio for each region and the radii ratios R_3/R_1 and R_3/R_2. The coefficients of equations 30 and 31 were calculated by numerical inversion of equations B19 to B40 of Appendix B by means of the F04AMF subroutine from the NAG Fortran Library. This solution has been tested by selecting appropriate

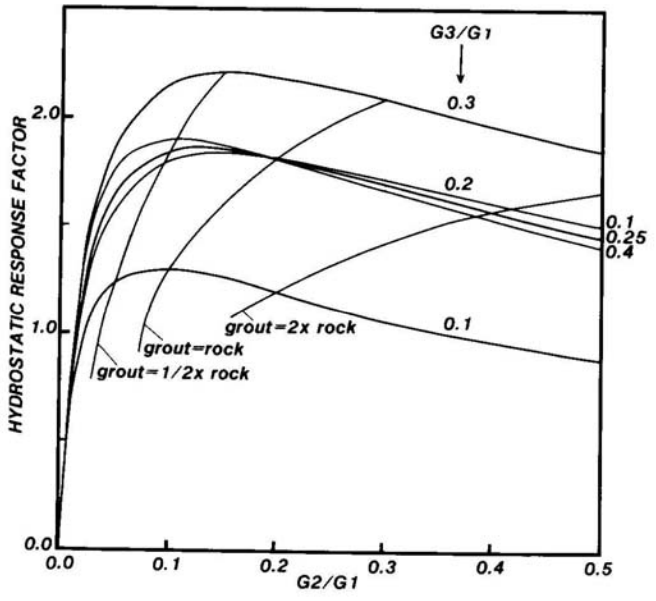

Figure 6

The effect of the grout rigidity (expressed as the ratio of grout rigidity to the instrument material rigidity) on the hydrostatic response of the two-ring model. Curves are shown for a common range of rock rigidities (again expressed as a ratio of the rock-to-instrument rigidities) and for Poisson ratios of the rock and grout equal to 0.25. A particular instrument geometry ($R_1 = 56$ mm, $R_2 = 62$ mm, $R_3 = 89$ mm) has been chosen for this example. The effect of the Poisson ratio of the grout is negligible and is shown by the three closely spaced curves ($\nu_2 = 0.1, 0.25, 0.4$) for the case of rock rigidity 0.2 of the instrument rigidity. It should also be noted that the response decreases for grout 'stronger' than the rock and increases marginally for grout 'softer' than the rock.

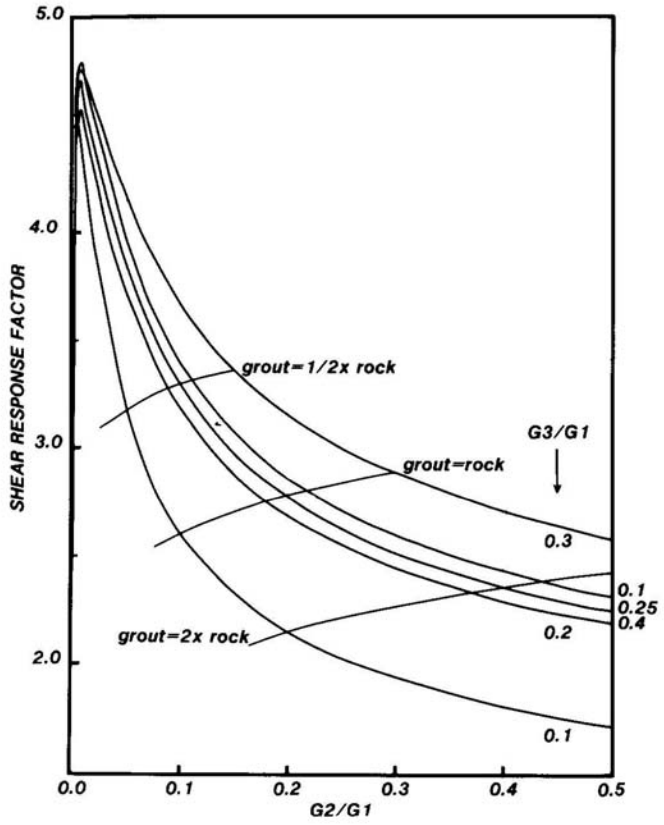

Figure 7

The effect of the grout rigidity (expressed as the ratio of grout rigidity to the instrument material rigidity) on the shear response of the two-ring model. Curves are shown for a common range of rock rigidities (expressed as a ratio of rock to instrument rigidities) and for Poisson ratios of the rock and grout equal at 0.25. Instrument geometry is as in Figure 6. The slight effect of the Poisson ratio of the grout is shown by the closely spaced curves ($\nu_2 = 0.1, 0.25, 0.4$) for the case of rock rigidity 0.2 of the instrument rigidity. Note that the response factor decreases rapidly if grout rigidity becomes significantly greater than rock rigidity. On this figure the actual response factor is critically dependent on instrument and hole geometry.

parameters to reduce it in all possible ways to the one-ring model and the empty borehole for comparison with the independently derived results for those models.

The effect of the grout rigidity on the response factors is shown in Figures 6 and 7 for several rock rigidities and for the instrument and borehole geometries encountered in typical borehole strain meter applications. Poisson ratios for the grout and the rock have been set equal at 0.25, except for the curves for $G_3/G_1 = 0.2$, where the effects of the Poisson ratio of the grout are shown to be small. As the grout rigidity (and therefore its bulk modulus) decreases, the hydrostatic response factor increases, to reach a maximum where the grout and rock rigidities are approximately equal. As the rock rigidity is increased, the response increases, and the maximum occurs for grout rigidity softer relative to the rock. The case for no grout is shown by the curve 'grout = rock' where, as expected, the effect of ν_2 disappears. A similar dependence on the grout rigidity is seen in the shear response factor, but with the

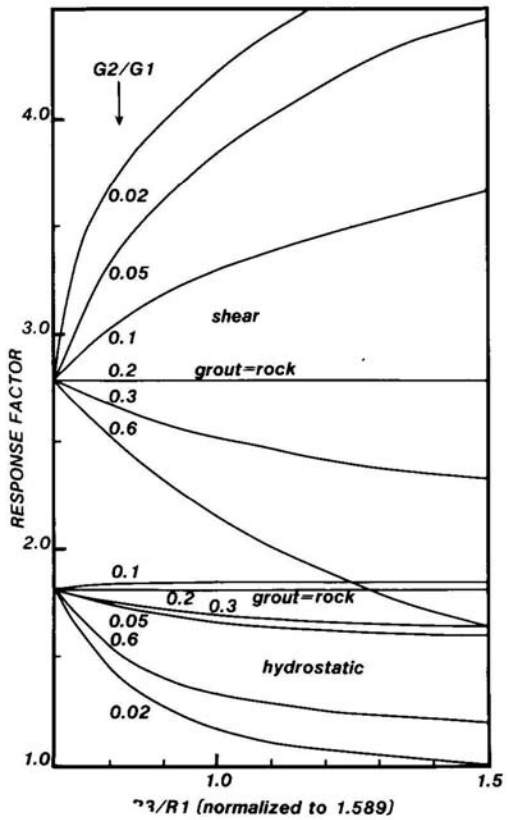

Figure 8

This figure illustrates the variation of the response factors with changes in the borehole radius, for constant instrument geometry ($R_2/R_1 = 1.107$) and constant rock rigidity ($G_3/G_1 = 0.2$ or $G_3 = 17$ GPa) for the two-ring model. The effect is shown for several values of the grout rigidity (expressed as the ratio of grout rigidity G_2 to instrument rigidity G_1). For 'softer' grouts large enhancements of the shear response occur as the borehole radius increases, due mainly to the coupling through of larger displacements to the fixed inner radius. The effect on the hydrostatic response is less, and no significant enhancement occurs. In both cases the responses tend to the one-ring model responses as the grout thickness decreases to zero (R_3/R_1 tends to R_2/R_1).

differences that the maximum gain is obtained for grout much less rigid than the rock and that the enhancement of the response compared with the grout-free case is greater than for the hydrostatic response. Large enhancements of the shear response over the hydrostatic response are possible for these low values of the grout rigidity, but it is probably inadvisable to use them in field instruments, since the response is highly dependent on the grout rigidity.

The effects on the hydrostatic and shear response factors of variations in the grout thickness while the instrument geometry is kept constant are shown in Figure 8 for several values of the grout rigidity. Here the rock rigidity is constant at 0.2 of the instrument rigidity, and ν_2 and ν_3 equal 0.25. Increasing the grout thickness has little effect for grout rigidity close to that of the rock, and decreases hydrostatic response for grout rigidity significantly different from that of the rock. The effect is much greater

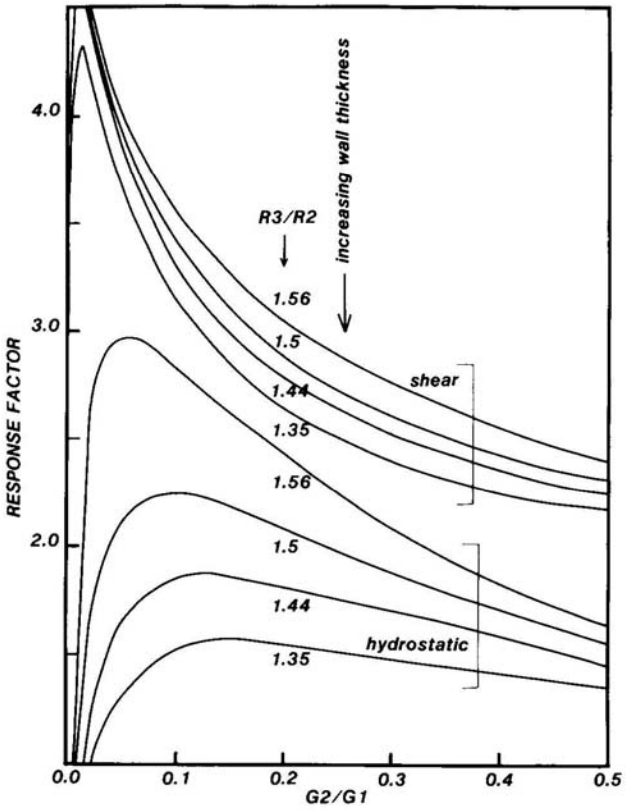

Figure 9

The effect on hydrostatic and shear responses of the two-ring model of varying the grout rigidity (expressed as the grout-to-instrument wall-rigidity ratio G_2/G_1) is shown with the borehole and inner instrument radii constant ($R_3 = 89$ mm, $R_1 = 56$ mm) is shown with the instrument wall thickness (indirectly expressed as the ratio R_3/R_2) a parameter. Rock rigidity is held constant at 0.2 of the instrument material rigidity, and Poisson ratios for the grout and rock are equal at 0.25. The curves can be compared with those of Figures 6 and 7.

for the shear response, with large enhancements for grout 'stronger' than the rock and reductions for the grout 'weaker'. These effects are enhanced as the grout thickness is increased.

Changing the instrument wall thickness while keeping the instrument inner radius and the borehole radius constant is of practical interest, because it is the one parameter over which there is some control in instrument design. The effects are best understood by first examining Figure 9, where the response factors are plotted as functions of the grout rigidity with the ratio R_3/R_2 as a parameter. A general conclusion is that decreasing the wall thickness increases the gains, with larger effects for 'softer' grout. By appropriate parameter selection significant enhancement of shear response over hydrostatic response can be obtained. In Figures 10 and 11 the hydrostatic and shear responses are given as functions of the ratio R_3/R_2 with G_2/G_1 as a parameter. Two limiting cases can be seen: first, where the instrument fills the hole ($R_3/R_2 = 1.0$), and

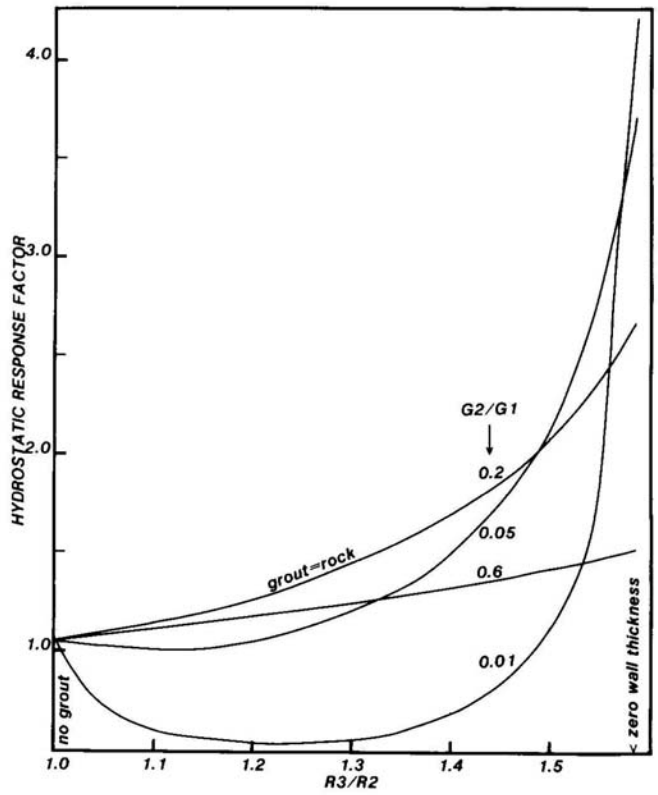

Figure 10

This figure shows the dependence of the hydrostatic response for the two-ring model on instrument wall thickness (expressed as R_3/R_2) for several values of the grout rigidity. The curves are for constant borehole and instrument inner radii ($R_3 = 89$ mm, $R_1 = 56$ mm) and constant rigidity of the rock of 17 GPa (0.2 of the instrument rigidity), and allow optimization of instrument wall thickness in a pre-existing borehole. Poisson's ratio for the grout and rock are equal at 0.25. Except for soft grout, where the effects are more complex, increasing the instrument wall thickness decreases the response. These results should be compared with those of Figure 11 for the shear response.

second, where the instrument wall thickness is zero. Both can be calculated and understood by the one-ring model with appropriate parameters.

Application to practical instruments

The accurate application of these results to borehole instruments requires that the following conditions be met.

1. The grout is 'welded' to the instrument outer wall and the borehole wall.
2. The instrument is central in the hole; eccentric location of the instrument in extreme cases will change the instrument response factors.
3. The hole and the instrument are cylindrical.
4. The region of rock around the instrument is representative and well coupled to the far-field strains of interest.

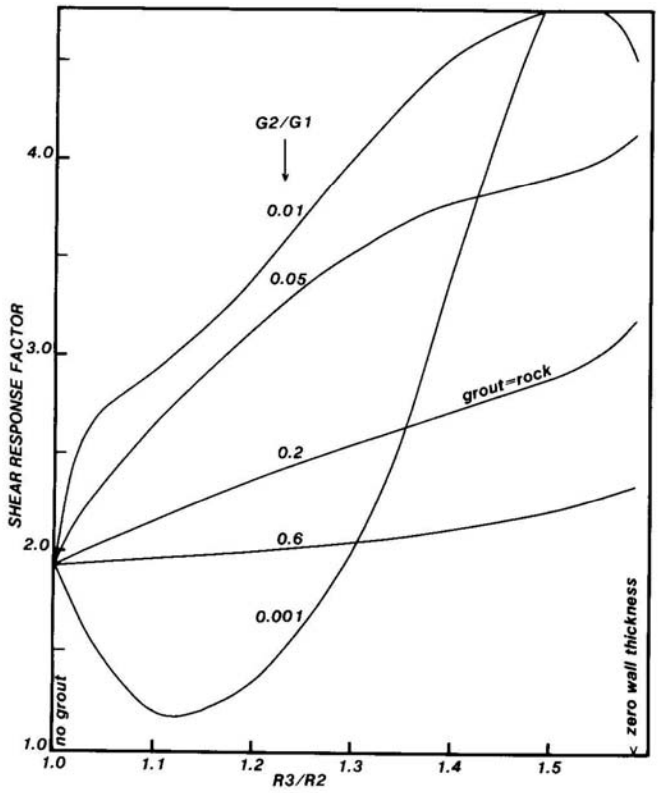

Figure 11
This figure shows the dependence of shear response for the two-ring model on instrument wall thickness for several values of the grout rigidity, for the parameters of Figure 10. Except for very soft grout, the effect of increasing the instrument wall thickness is to decrease the response.

5. The instrument is installed in a homogeneous, isotropic environment, and there are no significant strain gradients across the borehole.

6. The instrument measures radial displacement only of the inner instrument wall.

7. The strain changes encountered result from pure plane stress.

8. The host rock is linear if its elastic constants are determined from destressed core samples.

Even if these conditions are not met strictly, the results are useful in understanding the complex interaction of the components of an installed borehole instrument. Where the conditions are met, the results can be used to allow accurate measurements of hydrostatic and shear stress or strain changes in a horizontal plane, provided the elastic constants of the rock and the grout can be reliably measured from samples.

Conclusions

The foregoing series of graphical presentations illustrates the sensitivity of instrument strain response to various combinations of parameters available to the instru-

ment designer in the fabrication of an optimal instrument for a particular application. It is clear that an instrument implant cannot be optimised without adequate information on the basic elastic parameters of the host rock, so that core sampling of possible sites is essential in the production of a well matched instrument. The graphical presentations in some cases involve choice of particular parameters, so that the effect of a particular independent variable can be conveniently illustrated. This approach in no way limits the range of validity of the solutions presented, and the analytical solutions for each of the cases shown is readily available from the equations in the text or the appendices. The equations can easily be modified for applications involving plane strain.

Appendix A. The one-ring model

From equation 5.15 of SAVIN (1961) the constants a and b of equation 1 may be expressed as the following, where $N_1 = R_3/R_1$.

(A1) $$a = a_1(\chi_1 - 1) + b_{-1}N_1^2$$

(A2) $$b = a_3(\chi_1 - 3)N_1^{-2} + b_1 + a_{-1}(\chi_1 + 1)N_1^2 + b_{-3}N_1^4$$

The coefficients of these equations may be written as

(A3) $$a_{-1} = F_9(F_1 + F_8)$$

(A4) $$a_1 = F_2F_7[2F_1 - F_2(F_1 - F_5)]$$

(A5) $$a_3 = -F_9F_4(F_2 - 1)F_1$$

(A6) $$b_{-3} = -F_9(F_1 + F_4F_5)$$

(A7) $$b_{-1} = 2F_2a_1$$

(A8) $$b_1 = F_9F_2[F_1(4 - 3F_2) + F_8]$$

where

(A9) $$F_0 = G_3/G_1$$

(A10) $$F_1 = F_0 - 1$$

(A11) $$F_2 = N_1^2$$

(A12) $$F_3 = \chi_1F_0$$

(A13) $$F_4 = N_1^4$$

(A14) $$F_5 = 1 + F_3$$

(A15) $$F_6 = N_1^6$$

(A16) $$F_7 = 1 + \chi_3$$

(A17) $$F_8 = F_5F_6$$

(A18) $$F_9 = 2F_7/D_1$$

(A19) $$D_1 = (\chi_3 + F_0)F_2[F_1(3F_4 - 6F_2 + 4) + F_8] + (\chi_1F_0 - \chi_3)(F_1 + F_8)$$

Appendix B. The two-ring model

According to MUSKHELISHVILI (1953), the stress state and the displacements for the two-ring system can be solved in terms of two complex functions $\varphi(z)$ and $\psi(z)$, where $z = re^{i\theta}$. SAVIN shows that in the plate these functions have the following form (SAVIN, 1961, equations 5.2),

$$\varphi^3(z) = \varphi_0(z) + iC\sum_1^\infty \alpha_{-k}(R/z)^k \tag{B1}$$

$$\psi^3(z) = \psi_0(z) - iC\sum_1^\infty \beta_{-k}(R/z)^k \tag{B2}$$

where C is a constant, R is the hole radius, and $\varphi_0(z)$ and $\psi_0(z)$ are the stress functions for the plate when the hole is absent. They may be expressed (SAVIN, 1961, equation 5.1) as

$$\varphi_0(z) = iC\sum_1^m L_k(z/R)^k \tag{B3}$$

$$\psi_0(z) = -iC\sum_0^m M_k(z/R)^k \tag{B4}$$

For tension P applied along the X axis at infinity we have (SAVIN, 1961, equation 5.11):

$$\varphi_0(z) = (P/4)z \tag{B5}$$

$$\psi_0(z) = (-P/2)z \tag{B6}$$

so that

$$L_1 = (P/C)Ri(-\tfrac{1}{4}) \tag{B7}$$

$$M_1 = (P/C)Ri(-\tfrac{1}{2}) \tag{B8}$$

and the other terms L_k and M_k are zero.

For the rings (numbered 1 and 2 from the inside) the functions have the following form (SAVIN, 1961, equation 5.3):

$$\varphi^j(z) = iC\sum_{-\infty}^{\infty} A_k^j(z/R)^k \tag{B9}$$

$$\psi^j(z) = -iC\sum_{-\infty}^{\infty} B_k^j(z/R)^k \tag{B10}$$

In terms of these stress functions the displacements can be calculated (SAVIN, 1961, equation 5.7) by

$$(B11) \qquad U_r - iU_\theta = \frac{1}{2G}[\chi\bar{\varphi}(z) - \bar{z}\frac{d\varphi(z)}{dz} - \psi(z)]e^{i\theta}$$

which for the inner ring becomes

$$(B12) \qquad U_r^1 - iU_\theta^1 = \frac{1}{2G_1}[\chi_1\bar{\varphi}^1(z) - \bar{z}\frac{d\varphi^1(z)}{dz} - \psi^1(z)]e^{i\theta}$$

The stress can be calculated (SAVIN, 1961, equation 5.7) by

$$(B13) \qquad \sigma_r - i\tau_{r\theta} = \left(\frac{d\varphi(z)}{dz} + \overline{\frac{d\varphi(z)}{dz}}\right) - e^{2i\theta}\left(\bar{z}\frac{d^2\varphi(z)}{dz^2} + \frac{d\psi(z)}{dz}\right)$$

When the boundary conditions B14 to B18 are applied to the rings,

$$(B14) \qquad (\sigma_r^1 - i\tau_{r\theta}^1)_{R1} = 0$$
$$(B15) \qquad (\sigma_r^1 - i\tau_{r\theta}^1)_{R2} = (\sigma_r^2 - i\tau_{r\theta}^2)_{R2}$$
$$(B16) \qquad (\sigma_r^2 - i\tau_{r\theta}^2)_{R3} = (\sigma_r^3 - i\tau_{r\theta}^3)_{R3}$$
$$(B17) \qquad (U_r^1 - iU_\theta^1)_{R2} = (U_r^2 - iU_\theta^2)_{R2}$$
$$(B18) \qquad (U_r^2 - iU_\theta^2)_{R3} = (U^3 - iU_\theta^3)_{R3}$$

a set of 22 nonzero coefficients results, these being

$$A^j_{-1},\ A^j_1,\ A^j_2,\ A^j_3$$
$$B^j_{-3},\ B^j_{-2},\ B^j_{-1},\ B^j_0,\ B^j_1$$
$$\alpha_{-1}$$
$$\beta_{-3},\ \beta_{-2},\ \beta_{-1}$$
$$\text{for } j = 1, 2.$$

The real and imaginary parts of these coefficients are related by two sets of 22 linear nonhomogeneous equations arising from the boundary conditions. These equations are a special case of equations 5.8 of SAVIN (1961) for n rings, with errors removed. The rederived set for the two-ring case is given in equations B19 to B40, where $e_{ij} = G_i/G_j$.

$$(B19) \qquad 2A_1^1 - N_1{}^2B^1_{-1} = 0$$
$$(B20) \qquad 2A_1^1 - 2A_1^2 + N_2{}^2\bar{B}^1_{-1} - N_2{}^2\bar{B}^2_{-1} = 0$$
$$(B21) \qquad 2A_1^2 + \bar{B}^2_{-1} - \bar{\beta}_{-1} = 2L_1$$
$$(B22) \qquad e_{21}(\chi_1 - 1)A_1^1 - (\chi_2 - 1)A_1^2 - e_{21}N_2{}^2\bar{B}^1_{-1} + N_2{}^2\bar{B}^2_{-1} = 0$$
$$(B23) \qquad e_{32}(\chi_2 - 1)A_1^2 - e_{32}\bar{B}^2_{-1} + \bar{\beta}_{-1} = L_1(\chi_3 - 1)$$
$$(B24) \qquad A_2^1 + N_1{}^4\bar{B}^1_{-2} = 0$$

(B25) $A_2^1 - A_2^2 + N_2{}^4\bar{B}^1_{-2} - N_2{}^4\bar{B}^2_{-2} = 0$

(B26) $A_2^2 + \bar{B}^2_{-2} - \bar{\beta}_{-2} = 0$

(B27) $2e_{21}A_2^1 - 2A_2^2 - e_{21} - e_{21}N_2{}^2B_0^1 + N_2{}^2B_0^2 = 0$

(B28) $e_{21}\chi_1 A_2^1 - \chi_2 A_2^2 - e_{21}N_2{}^4\bar{B}^1_{-2} + N_2{}^4\bar{B}^2_{-2} = 0$

(B29) $e_{32}\chi_2 A_2^2 - e_{32}\bar{B}^2_{-2} + \bar{\beta}_{-2} = 0$

(B30) $2A_2^2 - B_0^2 = 0$

(B31) $N_1{}^4\bar{A}^1_{-1} + A_3^1 + N_1{}^6\bar{B}^1_{-3} = 0$

(B32) $-N_1{}^4\bar{A}^1_{-1} + 3A_3^1 - N_1{}^2B_1^1 = 0$

(B33) $N_2{}^4\bar{A}^1_{-1} + A_3^1 - N_2{}^4A^2_{-1} - A_3^2 + N_2{}^6\bar{B}^2_{-3} = 0$

(B34) $-N_2{}^4\bar{A}^1_{-1} + 3A_3^1 + N_2{}^4\bar{A}^2_{-1} - 3A_3^2 - N_2{}^2B_1^1 + N_2{}^2B_1{}^2 = 0$

(B35) $\bar{A}^2_{-1} + A_3^2 + \bar{B}^2_{-3} - \bar{\beta}_{-3} - \bar{\alpha}_{-1} = 0$

(B36) $-\bar{A}^2_{-1} + 3A_3^2 - B_1^2 + \bar{\alpha}_{-1} = -M_1$

(B37) $-e_{21}\chi_1 N_2{}^4\bar{A}^1_{-1} + e_{21}\chi_1 A_3^1 + N_2{}^4\bar{A}^2_{-1} - \chi_2 A_3^2 - e_{21}N_2{}^6\bar{B}^1_{-3} + N_2{}^6\bar{B}^2_{-3} = 0$

(B38) $e_{21}\chi_1 N_2{}^4\bar{A}^1_{-1} + 3e_{21}A_3^1 - \chi_2 N_2{}^4\bar{A}^2_{-1} - 3A_3^2 - e_{21}N_2{}^2B_1^1 + N_2{}^2B_1^2 = 0$

(B39) $-e_{32}\bar{A}^2_{-1} + e_{32}\chi_2 A_3^2 - e_{32}\bar{B}^2_{-3} + \bar{\beta}_{-3} + \bar{\alpha}_{-1} = 0$

(B40) $e_{32}\chi_2\bar{A}^2_{-1} + 3e_{32}A_3^2 - e_{32}B_1^2 - \chi_3\bar{\alpha}_{-1} = -M_1$

With equations B9 and B10 used in equation 12 and z set to $re^{i\theta}$, the radial displacement can be expressed in terms of these coefficients as the following, when $n = R/r$:

(B42)
$$U_r = \frac{1}{2G_1}\,\mathrm{Re}\Big[(-iC\chi_1)\Big(\bar{A}^1_{-1}ne^{i2\theta} + \frac{\bar{A}_1^1}{n} + \bar{A}_2^1\frac{e^{-i\theta}}{n^2} + \bar{A}_3^1\frac{e^{-i2\theta}}{n^3}\Big) - (iC)\Big(-A^1_{-1}ne^{-i2\theta} + \frac{A_1^1}{n} + 2A_2^1\frac{e^{i\theta}}{n^2} + 3A_3^1\frac{e^{2i\theta}}{n^3}\Big) + (iC)\Big(B^1_{-3}n^3e^{-2i\theta} + B^1_{-2}n^2e^{-i\theta} + B^1_{-1}n + B_0^1e^{i\theta} + B_1^1\frac{e^{2i\theta}}{n}\Big)\Big]$$

When equations B19 to B40 are inverted to give the coefficients in this equation, the only nonzero terms are found to be those independent of θ or those containing $\cos 2\theta$. Writing

(B43)
$$a_j^i = \frac{C}{PR}\mathrm{Im}(A_j^i)$$

$$b_j^i = \frac{C}{PR}\mathrm{Im}(B_j^i)$$

the radial displacement can be expressed as

(B44)
$$U_r = \frac{RP}{8G_1}\Big[\frac{4(1-\chi_1)a_1^1 - b^1_{-1}n}{n} + 4\Big(-a^1_{-1}n(1-\chi_1) + \frac{a_3^1}{n^3}(3-\chi_1) - b^1_{-3}n - \frac{b_1^1}{n}\Big)\cos 2\theta\Big]$$

For displacements evaluated at $r = R_1$ so that $n = N_1$ this reduces to

$$U_r = \frac{R_1 P}{8G_1}(a + b \cos 2\theta) \tag{B45}$$

where

$$a = 4\left[\frac{(1-\chi_1)}{N_1} a_1^1 - b_{-1}^1 N_1{}^2\right]$$

$$b = 4\left[-a_{-1}^1 N_1{}^2(1+\chi_1) + \frac{a_3^1}{N_1{}^2}(3-\chi_1) - b_{-3}^1 N_1{}^4 - b_1^1\right].$$

References

Amadei, B. (1983), *Rock anisotropy and the theory of stress measurements*, Springer-Verlag.

Gladwin, M. T. (1984), *High precision multi-component borehole deformation monitoring*, Rev. Sci. Instr. 55, No. 12, 2011–2016.

Jaeger, J. C. and Cook, N. G. W. (1976), *Fundamentals of rock mechanics*, 2nd ed. Chapman and Hall.

Muskhelishvili, N. I. (1953), *Some basic problems of the mathematical theory of elasticity*, Noordhoff Ltd., Groningen, Holland. Trans. J. R. M. Radok.

Sacks, I. S., Suyehiro, S., Evertson D. W. and Yamagishi, Y. (1971), *Sacks-Evertson strainmeter, its installation in Japan and some preliminary results concerning strain steps*, Papers Meterol. Geophys. *22*, Nos. 3–4, 195–208.

Sakata, S., Shimada, S. and Noguchi, S. (1982), *Development of new-type three-component borehole strainmeters*, Proc. 3rd Joint Panel Mtg. U.J.N.R. Panel Earthquake Prediction Technology, pp. 234–248.

Savin, G. N. (1961), *Stress concentration around holes*, Pergamon Press. Transl. W. Johnson.

(Received 19th November 1984, revised 12th February 1985, accepted 12th February 1985)